Geological Magazine

www.cambridge.org/geo

Original Article

Cite this article: Satpathy RK, Steinke S, and Singh AD (2020) Monsoon-induced changes in surface hydrography of the eastern Arabian Sea during the early Pleistocene. *Geological Magazine* **157**: 1001–1011. https://doi.org/10.1017/S0016756819000098

Received: 18 July 2018
Revised: 24 January 2019
Accepted: 24 January 2019
First published online: 8 March 2019

Keywords:
Arabian Sea; early Pleistocene; hydrography; IODP Site U1457; monsoon; planktic foraminifera

Author for correspondence:
Arun Deo Singh,
Email: arundeosingh@yahoo.com

© Cambridge University Press 2019.

CAMBRIDGE
UNIVERSITY PRESS

Monsoon-induced changes in surface hydrography of the eastern Arabian Sea during the early Pleistocene

Rajeev Kumar Satpathy[1], Stephan Steinke[2,3] and Arun Deo Singh[1]

[1]Center of Advanced Study in Geology, Banaras Hindu University, Varanasi, India; [2]MARUM – Center for Marine Environmental Sciences, University of Bremen, Bremen, Germany and [3]Department of Geological Oceanography & State Key Laboratory of Marine Environmental Science, Xiamen University, Xiamen, China

Abstract

Upper water column dynamics in the eastern Arabian Sea were reconstructed in order to investigate changes in the activity of the South Asian / Indian monsoon during the early Pleistocene (*c.* 1.5–2.7 Ma). We used planktic foraminiferal assemblage records combined with isotopic ($\delta^{18}O$ and $\delta^{13}C$) data, Mg/Ca-based sea surface temperatures and seawater $\delta^{18}O$ records to estimate changes in surface water conditions at International Ocean Discovery Program (IODP) Site U1457. Our records indicate two distinct regimes of monsoon-induced changes in upper water structure during the periods *c.* 1.55–1.65 Ma and *c.* 1.85–2.7 Ma. We infer that a more stratified upper water column and oligotrophic mixed layer conditions prevailed during the period 1.85–2.7 Ma, which may be due to overall weaker South Asian / Indian winter (NE) and summer (SW) monsoon circulations. The period 1.55–1.65 Ma was characterized by enhanced eutrophication of the mixed layer, which was probably triggered by intensified winter (NE) monsoonal winds. The long-term trend in hydrographic changes during 1.55–1.65 Ma appears to be superimposed by short-term variations, probably reflecting glacial/interglacial changes. We suggest that an intensification of the South Asian / Indian winter monsoon circulation occurred between ~1.65 Ma and 1.85 Ma, which is most likely due to the development of strong meridional and zonal atmospheric circulations (i.e. Walker Circulation and Hadley Circulation) because of strong equatorial East–West Pacific temperature gradients.

1. Introduction

The South Asian or Indian monsoon system represents one of the basic elements of global atmospheric circulation. However, little is known about its evolution and variability over long periods of geologic time. Previous palaeoceanographic and palaeoclimatic reconstructions from the western and northern Arabian Sea, using planktic foraminiferal assemblages and geochemical proxies, provided deep insights into South Asian / Indian monsoon variability on long- to short-term timescales (orbital to sub-orbital and centennial to sub-centennial scales) (e.g. Clemens *et al.* 1991; Anderson & Prell, 1993; Vénec-Peyré *et al.* 1995; Naidu & Malmgren, 1996; Reichart *et al.* 1998; Schulz *et al.* 1998; von Rad *et al.* 1999; Schulte & Müller, 2001; Jung *et al.* 2002; Gupta *et al.* 2003; Ivanova *et al.* 2003; Ivanochko *et al.* 2005). Earlier studies suggested that fossil planktic foraminiferal assemblages in the eastern Arabian Sea (EAS) record primarily winter monsoon induced changes in surface water oceanographic conditions (Singh *et al.* 2006, 2011, 2018), because winter monsoon winds play a dominant role in surface hydrography and biological productivity. Most of the previous palaeoceanographic reconstructions based on planktic foraminiferal assemblages and geochemical proxies (e.g. stable isotopes and Mg/Ca-based sea surface temperature (SST)) from the EAS mainly focused on the last glacial–interglacial cycle (Cayre & Bard, 1999; Thamban *et al.* 2001; Ivanova *et al.* 2003; Pattan *et al.* 2003; Banakar *et al.* 2005; Chodankar *et al.* 2005; Guptha *et al.* 2005; Singh *et al.* 2006, 2011, 2018; Anand *et al.* 2008). However, no record of millennial- to orbital-scale variations from this region is currently available extending beyond the last glacial–interglacial cycle, particularly for the early Pleistocene, which has been suggested as a period when a major reorganization of atmospheric circulation from a weak to a strong zonal Walker circulation took place (Etourneau *et al.* 2010). For that reason, sediment records retrieved at IODP Site U1457 in the Laxmi Basin of the EAS provide an opportunity to reconstruct the history of oceanographic and monsoon variations on tectonic, orbital to sub-orbital timescales further back in geological time (Pandey *et al.* 2015).

Here, we present planktic foraminiferal assemblage records together with stable carbon and oxygen isotopes, Mg/Ca-based SSTs and seawater $\delta^{18}O$ estimates in order to decipher changes in the regional surface hydrography and productivity in the EAS during the early Pleistocene and, hence, changes in strength of the South Asian / Indian monsoonal circulation. This study also

https://doi.org/10.1017/S0016756819000098 Published online by Cambridge University Press

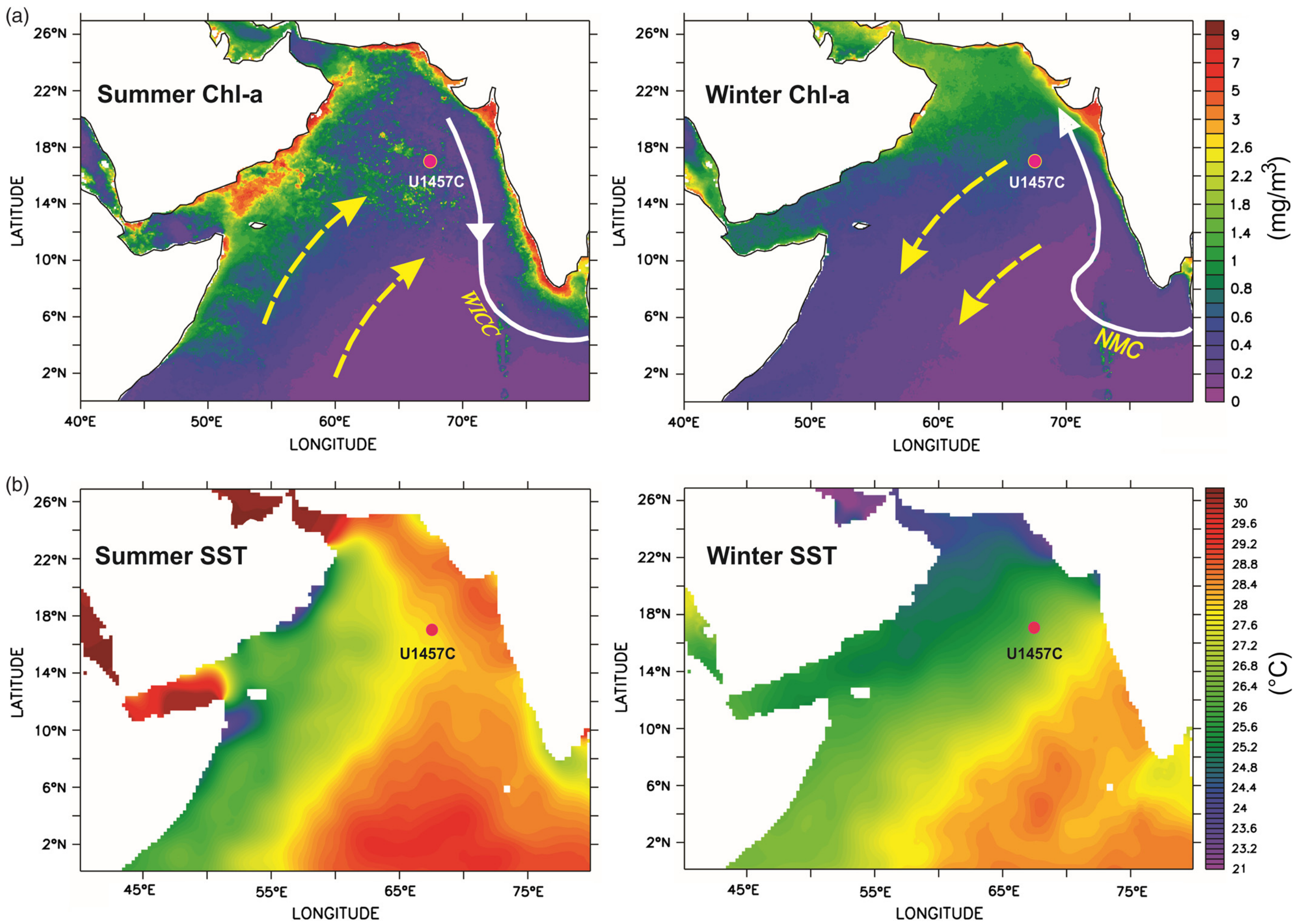

Fig. 1. Map showing the location of IODP Site U1457. Schematic representation of dominant wind directions (dashed yellow lines) and main surface ocean circulation (white lines) in the Arabian Sea during the monsoons (as inferred from Schott & McCreary, 2001; Singh *et al.* 2011; Cabarcos *et al.* 2014). Map indicates chlorophyll concentration (a) and sea surface temperature (SST) (b) during the summer and winter monsoons (sources: Chl a: NASA/SeaWiFS; SST: US National Oceanic and Atmospheric Administration). WICC: West Indian Coastal Current; NMC: Northeast Monsoon Current.

aims to examine possible atmosphere–ocean–climate linkages between the South Asian / Indian monsoon system and low- and high-latitude climate components.

2. Study area

The climate and surface hydrography in the Arabian Sea are primarily controlled by the seasonally reversing South Asian / Indian monsoon wind patterns (Fig. 1). The monsoon winds produce distinct seasonal and spatial variations in surface ocean hydrography, circulation, nutrient distribution and productivity (e.g. Banse, 1987; Brock *et al.* 1994; Luis & Kawamura, 2004). The advection of upwelled water from the western Arabian Sea during the summer SW monsoon season (June to September) and convective mixing during the winter NE monsoon (November–February) modulate biological productivity in the EAS. During the summer monsoon season, a clockwise circulation develops in the Arabian Sea (Schott, 1983), and the eastern branch of this anticyclonic circulation forms the West India Coastal Current (WICC) (Shetye *et al.* 1991) in the EAS. The equatorward-flowing WICC in summer carries high-salinity waters from the northern Arabian Sea towards the south (Prasanna Kumar *et al.* 2004). As the wind system reverses during the winter, the WICC starts flowing northward against the alongshore component of the wind stress (Shetye *et al.* 1991) carrying the low salinity waters from the Bay of Bengal (Prasanna Kumar *et al.* 2004). The dry northeasterly winter monsoon winds cause cooling of surface waters and vertical mixing with an injection of nutrient-rich subsurface waters into the photic zone (Banse, 1987; Lévy *et al.* 2007; Koné *et al.* 2009). This results in an increase in primary productivity in the northeastern and EAS (Banse & McClain, 1986; Madhupratap *et al.* 1996). The seasonally reversing winds also modulate the mixed layer depth (MLD) in the region (Banse, 1984). Recent studies have shown spatio-temporal variability of physical and biological parameters of MLD in the EAS (Shankar *et al.* 2015; Vijith *et al.* 2016). These studies suggest inhibition of MLD deepening in the south of the EAS due to advection of low-salinity water carried by the poleward-flowing WICC (Vijith *et al.* 2016). This in turn inhibits the entrainment of nutrients into the mixed layer, resulting in low chlorophyll concentration in the southern part of EAS (Vijith *et al.* 2016). Satellite-derived chlorophyll data reveals a regional difference in chlorophyll concentration within the EAS during winter, with high concentration in the northern EAS (Banse & McClain, 1986).

IODP Site U1457 in the Laxmi Basin is located at the eastern periphery of the oligotrophic part of the central Arabian

https://doi.org/10.1017/S0016756819000098 Published online by Cambridge University Press

Sea (Fig. 1). A subtle increase in productivity at the site during the summer monsoon season might be related to the advection of nutrient-rich upwelling filaments from the western Arabian Sea and/or to a higher supply of nutrients because of increased fluvial runoff into the EAS during the rainy summer monsoon season. On the contrary, an increase in productivity as revealed by the chlorophyll concentration data and cooler SST is recorded during the winter season. Annual primary productivity in the vicinity of the IODP Site U1457 is estimated to be lower (~166 g C m^{-1} a^{-1}), as compared to the northern and western Arabian Sea (~230–250 g C m^{-1} a^{-1}) (Madhupratap *et al.* 1996; Rixen *et al.* 2000; Ivanova *et al.* 2003). The MLD in winter is reported to be slightly deeper (60–80 m) than during the summer (40–80 m) (Rao *et al.* 1989; Madhupratap *et al.* 1996).

3. Material and methods

3.a. Site description and age model

IODP Site U1457 (17° 9.9486′ N, 67° 55.8121′ E; water depth 3534 m) is located within the Laxmi Basin in the EAS, ~491 km from the Indian coast and ~750 km from the present-day Indus River mouth (Fig. 1; Pandey *et al.* 2015). The Indus River is the major source of sediment supply to the Laxmi Basin (Pandey *et al.* 2015). Minor contributors of sediment to the Laxmi Basin are rivers flowing through the Western Ghats of India, mainly the Narmada and Tapti. Three holes were drilled at this site. The sedimentary section from 346 to 426 mbsf (metres below the seafloor) at Hole U1457C was selected for the present study. Sedimentation rates at Hole U1457C range from ~4 cm ka^{-1} in the lower part of the examined section to ~58 cm ka^{-1} in the upper part of the section, probably because of its location in the distal Indus fan (Pandey *et al.* 2016). Higher sedimentation rates in the upper part of the section might be attributed to a higher supply from the Indus around that time. The sediment consists mainly of foraminifera-rich nannofossil ooze, interbedded with silty clay and sandy silt layers. Sandy silt layers characterized by terrestrial detrital sediment are interpreted as turbidites (Pandey *et al.* 2015). The age model of the examined section is based on four calcareous nannofossil biostratigraphic datums (Pandey *et al.* 2015; Table 1). A short interval (~0.45 Ma) of non-deposition between 403.83 mbsf and 415.35 mbsf has been suggested based on biostratigraphic and lithological shipboard findings (see Pandey *et al.* 2016 for details). However, the available biochronological datums are not sufficient to confirm this hiatus.

3.b. Analytical methods

In total, 268 samples at 20 cm regular intervals were analysed for planktic foraminiferal assemblages. Dried samples were washed through wet sieving over a 63 µm sieve, following conventional processing technique. Residues (>63 µm) were dry sieved over a 125 µm sieve. We generated planktic foraminiferal census data from an aliquot of 250–300 specimens of the >125 µm size fraction of each sample. Those samples containing a low number of planktic foraminifera tests were used completely for counting. For species identification, the taxonomic concepts of Kennett & Srinivasan (1983) and Hemleben *et al.* (1989) were followed. Based on the census counts, the absolute abundance of each species was estimated (number of specimens / g dry sediment >125 µm).

Planktic foraminifera respond rapidly to changes in surface hydrography and primary productivity induced by variation in seasonal monsoon wind circulation, as reflected by variations in species abundance and chemical composition of their tests (e.g. Hutson & Prell, 1980; Steens *et al.* 1992; Peeters & Brummer, 2002; Anand *et al.* 2008). Therefore, planktic foraminiferal assemblages in sediment have great potential for reconstructing past surface ocean conditions (e.g. Ravelo *et al.* 1990; Kroon *et al.* 1991; Singh *et al.* 2006, 2018). We examined variations of foraminiferal proxies (absolute abundances of ecologically sensitive species and mixed layer eutrophic and oligotrophic species abundance ratio) to understand the temporal variability of the surface water hydrography, viz. stratification, vertical mixing and nutrient conditions in response to changes in the intensity of the seasonal monsoon circulation. The abundance ratio of *Globigerina bulloides* to *Globigerinoides ruber* is used as a proxy for palaeo-productivity variation associated with seasonal upwelling and/or vertical mixing versus stratification of upper water column (Conan & Brummer, 2000; Singh *et al.* 2011). The advantage of this palaeo-productivity proxy is that it is unaffected by dissolution artefacts in the sediment, as both species are equally sensitive to dissolution (Cullen & Prell, 1984; Conan *et al.* 2002). Hence, *G. bulloides* / *G. ruber* ratio is a robust proxy and this has been used previously for palaeoceanographic reconstructions in the EAS (Singh *et al.* 2006, 2011, 2018).

As the site lies above the modern calcium carbonate compensation depth (CCD), dissolution of calcite tests is expected to be minimal. Nevertheless, the degree of preservation of planktic foraminiferal assemblage has been evaluated by the record of absolute abundance ratio of common solution-susceptible species to solution-resistant species (Fig. 2). We also determined the dissolution index (DI) (number of resistance species tests / total number of common species tests × 10, following Berger (1973)) (Fig. 2).

Isotope analyses of *Globigerinoides sacculifer-quadrilobatus* of the 250–350 µm fraction were performed at MARUM, University of Bremen, on Finnigan MAT 251 mass spectrometers with Kiel I or Kiel III devices. Isotope values were calibrated against the international Vienna Pee Dee Belemnite (VPDB) standard. The internal carbonate standard is a Solnhofen Limestone, which is calibrated to the National Bureau of Standards (NBS) 19 standard. The long-term analytical precision was better than ±0.07 ‰.

SST was reconstructed based on shell Mg/Ca of the planktic foraminiferal species *G. sacculifer-quadrilobatus*. For each sample, *c.* 30–40 specimens of *G. sacculifer-quadrilobatus* were picked out of the 250–350 µm fraction. Foraminiferal tests were cleaned in successive steps following the cleaning protocol developed by Barker *et al.* (2003) and analysed with an inductively coupled plasma optical emission spectrometer (ICP-OES; Agilent Technologies, 700 Series with autosampler ASX-520 Cetac and micro-nebulizer) at MARUM – Center for Marine Environmental Sciences, University of Bremen, Germany. Instrumental precision of the ICP-OES was examined by analysis of an in-house standard solution with a Mg/Ca of 2.93 mmol mol^{-1} after every five samples with a long-term average of 2.94 mmol mol^{-1} (long-term standard deviation of 0.062 mmol mol^{-1}). To allow inter-laboratory

Table 1. Calcareous nannofossil datums used for age model of the examined section of Site U1457

Nannofossil datum	Age (Ma)	Base depth (m)	Top depth (m)
T *Discoaster pentaradiatus*	2.39	413.42	415.35
T *Discoaster brouweri*	1.93	391.1	403.83
B *Gephyrocapsa spp. >4 µm*	1.73	376.03	391.1
B *Gephyrocapsa spp. >5.5 µm*	1.62	356.6	363.55

https://doi.org/10.1017/S0016756819000098 Published online by Cambridge University Press

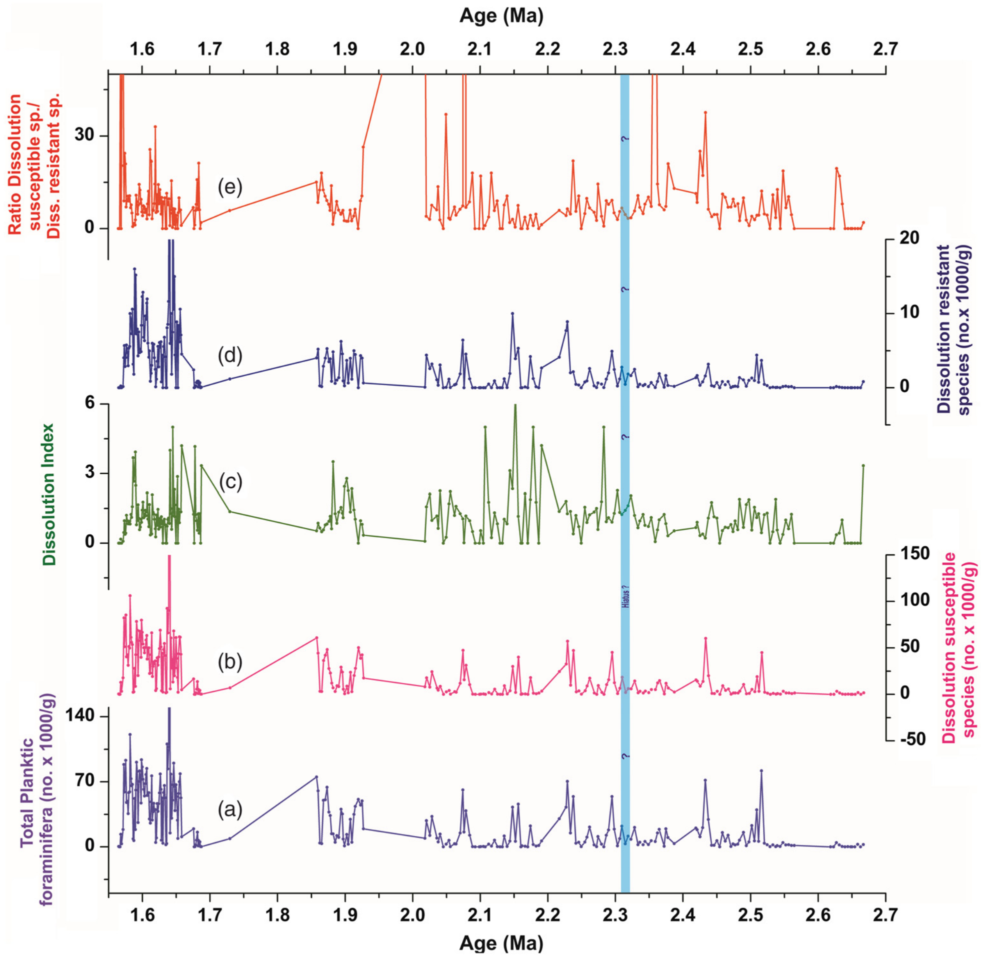

Fig. 2. Records of (a) total planktic foraminifera (no. × 1000 g^{-1}), (b) dissolution-susceptible species (no. × 1000 g^{-1}), (c) dissolution index (Berger, 1973), (d) dissolution-resistant species (no. × 1000 g^{-1}), (e) absolute abundance ratio of dissolution-susceptible species and dissolution-resistant species from IODP Hole U1457C.

comparison, we analysed an international limestone standard (ECRM752-1) with a reported Mg/Ca of 3.75 mmol mol^{-1}. The long-term average of the ECRM752-1 standard, which is routinely analysed twice before each batch of 50 samples in every session, is 3.78 mmol mol^{-1} ($1\sigma = 0.066$ mmol mol^{-1}). Mn/Ca, Fe/Ca and Al/Ca were determined together with Mg/Ca because clay contamination and the occurrence of syn-sedimentary and post-depositional Mn-oxide precipitates and Mn-rich carbonate coatings can exert a significant control on Mg/Ca ratios, resulting in elevated Mg/Ca ratios and, by inference, overestimated SSTs. Our results indicate no significant Mg contributions by Mn oxides or Mn-rich carbonates or clays because ratios for Mn/Ca and Fe/Ca were <0.1 mmol mol^{-1}, and not detectable for Al/Ca. The Mg/Ca ratios are not affected by the occurrence of post-depositional and syn-sedimentary precipitated Mn oxide and Mn-rich carbonate coatings, or by post-depositional partial dissolution. The *G. sacculifer-quadrilobatus* Mg/Ca estimates were converted to SSTs using the multiple-species equation of Anand *et al.* (2003) (Mg/Ca (mmol mol^{-1}) = 0.347 exp (0.09 SST)). The errors of the temperature reconstructions are estimated by propagating the errors introduced by the Mg/Ca measurements and the Mg/Ca temperature calibration (see Mohtadi *et al.* 2014). The resulting errors for *G. sacculifer-quadrilobatus* are on average 1.08 °C.

Seawater $\delta^{18}O$ (a proxy for salinity) was calculated by removing the temperature-driven component of changes in the $\delta^{18}O$ *G. sacculifer-quadrilobatus* record using the temperature–$\delta^{18}O$ seawater relationship given by Bemis *et al.* (1998) ($\delta^{18}O_{seawater} = (T - 16.5 + 4.8 * \delta^{18}O_{calcite})/4.8 + 0.27$). The component of seawater $\delta^{18}O$ that is attributed to changes in the local hydrology was then calculated by subtracting the influence of continental ice volume taken from Bintanja & van de Wal (2008).

4. Results

4.a. Planktic foraminiferal assemblages

The planktic foraminiferal assemblages recorded in this study comprise a total of 35 species, of which the most abundant are *Globigerina bulloides*, *Globigerinoides ruber*, *Globigerinita glutinata*, *Globigerinoides trilobus*, *Globigerinoides sacculifer*, *Neogloboquadrina dutertrei* and *Pulleniatina obliquiloculata*. Temporal variations in absolute abundances of these species are presented in Figure 3. The absolute abundance of total planktic foraminifera (number per g sediment >125 µm) varies between 0 and 99,000 specimens, with significantly lower abundances between 1.85 Ma and 2.7 Ma, followed by a prominent shift to higher values after 1.65 Ma (Fig. 2). Absolute abundances of the seven most dominant species remained low until 1.85 Ma and increased during the period 1.55–1.65 Ma (Fig. 3). *G. glutinata* is the most abundant species of the assemblage, followed by

https://doi.org/10.1017/S0016756819000098 Published online by Cambridge University Press

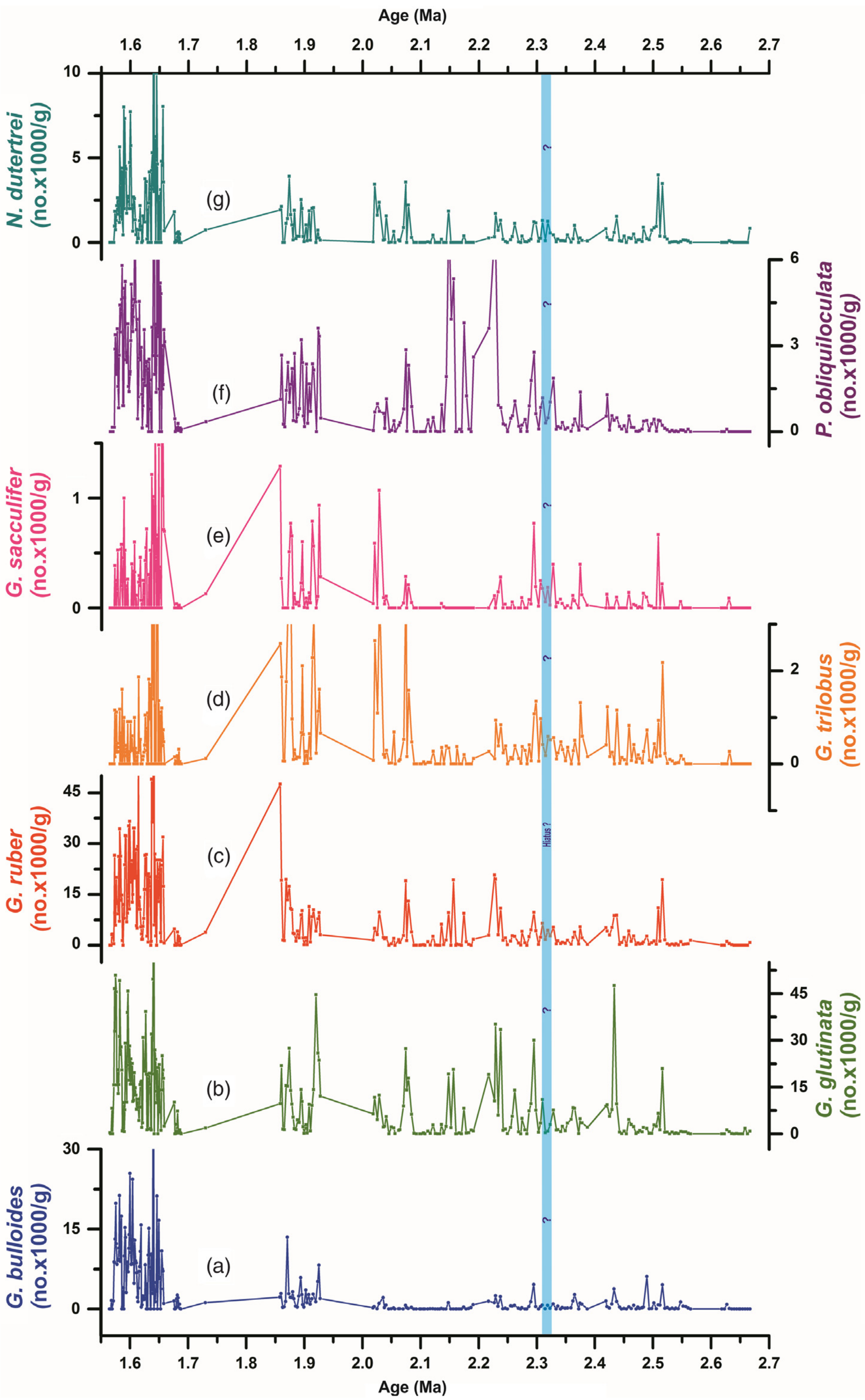

Fig. 3. Absolute abundances of planktic foraminifera: (a) *G. bulloides*, (b) *G. glutinata*, (c) *G. ruber*, (d) *G. trilobus*, (e) *G. sacculifer*, (f) *P. obliquiloculata*, (g) *N. dutertrei*.

G. ruber, *G. bulloides*, *N. dutertrei*, *P. obliquiloculata*, *G. trilobus* and *G. sacculifer* (in decreasing order of absolute abundances). The interval prior to 1.85 Ma is characterized by an overall low abundance of planktic foraminifera, with very low occurrence of *G. bulloides* and *N. dutertrei*. Between 1.55 Ma and 1.65 Ma, high absolute abundances of *G. bulloides* and *G. glutinata* are recorded. Relative abundance records of *G. glutinata* and *G. bulloides* in general reflect an opposite pattern to *G. ruber* (Fig. 5 below). The foraminiferal assemblages comprise both mixed layer eutrophic (*G. bulloides*, *G. glutinata*) and oligotrophic (*G. ruber*, *G. sacculifer*, *G. trilobus*) species. Temporal variation patterns in abundance ratios of mixed layer eutrophic to oligotrophic species (a proxy for mixed layer trophic conditions) and *G. bulloides* to *G. ruber* (a proxy for surface water stratification) show major

https://doi.org/10.1017/S0016756819000098 Published online by Cambridge University Press

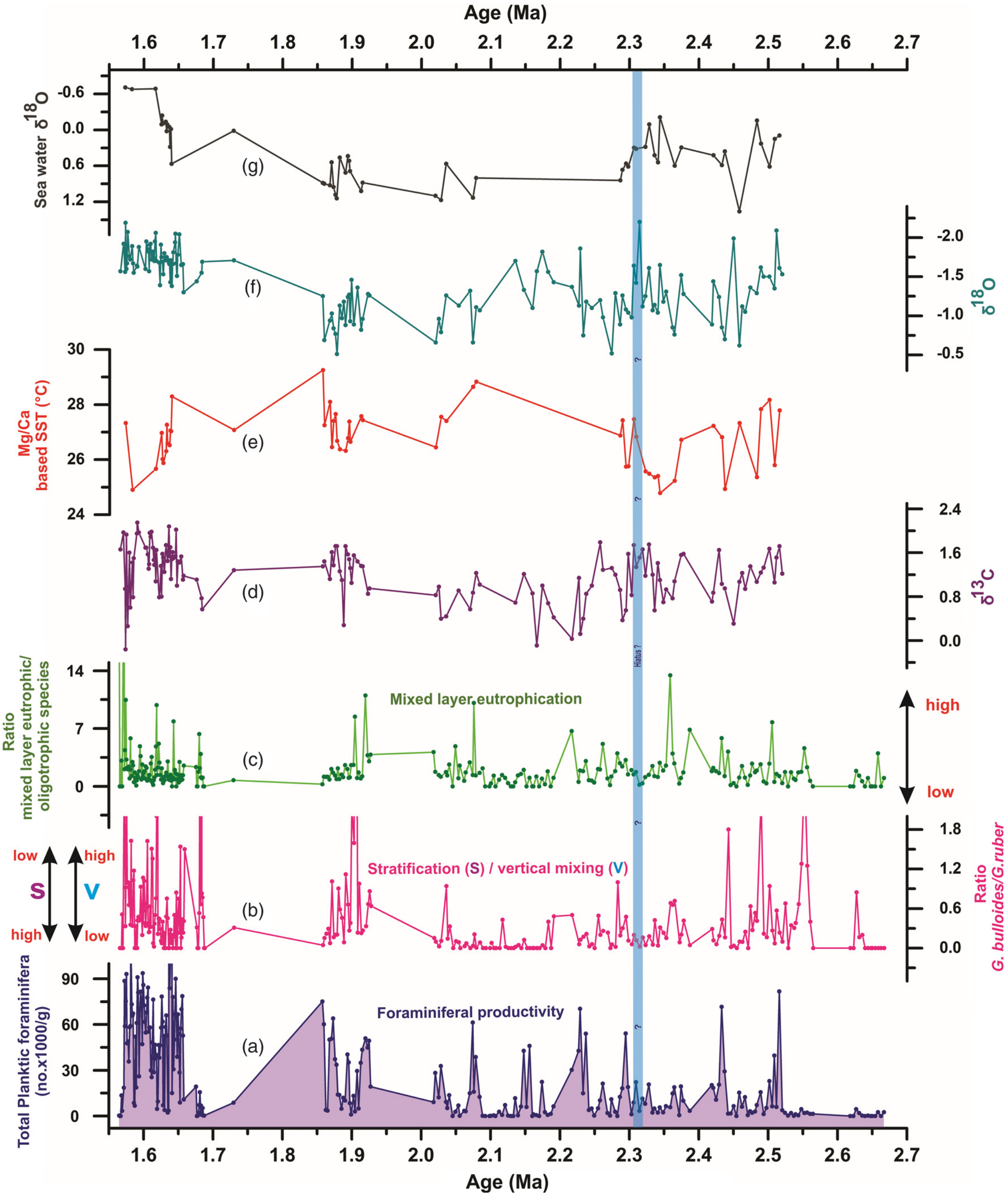

Fig. 4. Foraminiferal, oxygen and carbon isotope, and SST records. (a) Total planktic foraminiferal abundance, (b) absolute abundance ratio of *G. bulloides* and *G. ruber*, (c) absolute abundance ratio of mixed layer eutrophic and oligotrophic species, (d) $\delta^{13}C$ (‰), (e) Mg/Ca-based SST record in °C, (f) $\delta^{18}O$ record of *G. sacculifer-quadrilobatus*, (g) seawater $\delta^{18}O$.

changes between 1.55 Ma and 1.65 Ma (Fig. 4 below). Before 1.85 Ma, the values of these proxy records are generally low as compared to the younger interval (1.55–1.65 Ma). The temporal variation pattern of the *G. bulloides* / *G. ruber* ratio broadly follows that of mixed layer eutrophic/oligotrophic species abundance ratio.

4.b. Stable oxygen, carbon isotopes, Mg/Ca-based SST estimates and seawater $\delta^{18}O$ estimates

The oxygen isotope record of the surface planktic foraminifera *G. sacculifer-quadrilobatus* shows significant variations, with a maximum value of −0.51 ‰ and a minimum value of −2.18 ‰ (Fig. 4). However, the isotope record reflects a different pattern of variations at 1.55–1.65 Ma and 1.85–2.7 Ma. During the period 1.55–1.65 Ma, most of the samples show lighter values (<−1.50 ‰) with a mean value of −1.74 ‰. $\delta^{18}O$ in this time interval varies between −1.38 ‰ and −2.19 ‰. In contrast, $\delta^{18}O$ values during the period 1.85–2.7 Ma, except for a few samples, are relatively heavier (>1.50 ‰) with an average value of −1.21 ‰. The difference of 0.53 ‰ between the average values of the two time slices is intriguing. The carbon isotope record also shows major variations

https://doi.org/10.1017/S0016756819000098 Published online by Cambridge University Press

during the two time intervals. The average value $\delta^{13}C$ between 1.85 Ma and 2.7 Ma is lighter (1.09 ‰), as compared to that between 1.55 Ma and 1.65 Ma (1.21 ‰). The $\delta^{13}C$ varies between −0.16 ‰ and 2.14 ‰, with significantly higher values between 1.55 Ma and 1.65 Ma.

The *G. sacculifer-quadrilobatus* Mg/Ca-based SST record reveals that sea surface temperature at the examined site varies between 24.8 °C and 29.2 °C during the investigated time period 1.55–2.7 Ma (Fig. 4). The record of seawater $\delta^{18}O$ estimates shows lighter values between 1.55 Ma and 1.65 Ma compared with the time period prior to 1.85 Ma, which is suggested to reflect a period of stronger monsoonal rainfall and/or riverine runoff.

5. Discussion

5.a. Preservation vs dissolution of planktic foraminifera

Because the examined site is located in the distal Indus fan, it is assumed that the foraminiferal abundance record is influenced by terrestrial input resulting in dilution of pelagic sediment components deposited at the sea floor (e.g. Singh *et al.* 2006). Hence, the interval prior to 1.85 Ma, which is characterized by an overall low abundance of planktic foraminifera, may represent a period of higher supply of terrigenous-siliciclastic material to IODP Site U1457. We therefore suggest that the assemblage within a few intervals in the lower section (1.85–2.7 Ma) that have very low planktic foraminifera abundances is probably related to the dilution of faunal population caused by high terrestrial input to our site. In addition, deepening of the carbonate lysocline in the past may have influenced the preservation of foraminiferal tests. Dissolution effects on foraminiferal tests during these intervals can also not be ruled out, as is evident from the DI record (Fig. 2). Moreover, the intervals with moderate to high abundances, although not as high as recorded in the younger interval between 1.55 Ma and 1.65 Ma, probably suggest better preservation of foraminiferal tests and minimum sediment dilution. The preservation of foraminifera was good, along with minimal dilution of sediment in the period between 1.55 Ma and 1.65 Ma.

5.b. Seasonal monsoon wind induced changes in surface water hydrography and productivity

The planktic foraminiferal assemblages, oxygen and carbon isotopes and Mg/Ca SST records obtained for the studied section at IODP Site U1457 reveal significant fluctuations in the surface hydrography and productivity conditions in the Laxmi Basin during the early Pleistocene between *c.* 1.5 Ma and 2.7 Ma. Our proxy records indicate two distinct regimes of monsoon wind induced changes in upper water column structure and surface productivity during the periods 1.85–2.7 Ma and 1.55–1.65 Ma. We suggest that general low absolute abundances of the planktic foraminifera species *G. glutinata*, *G. bulloides* and *N. dutertrei* between 1.85 Ma and 2.7 Ma indicate stratified, nutrient-poor (oligotrophic) and low-productivity surface water conditions. This assertion is based on the fact that today *G. glutinata*, *G. bulloides* and *N. dutertrei* are associated with high-productivity environments in the Arabian Sea. *G. glutinata* feeds upon diatoms and is considered to be linked with the winter diatom bloom in the NE Arabian Sea because of vertical mixing and entrainment of nutrients into the mixed layer (Schulz *et al.* 2002). Therefore, high (low) abundances of this species are suggestive of high (low) surface water productivity conditions, related to winter monsoonal wind induced overturning. *G. bulloides* is considered as a eurythermal species occurring abundantly in cold, nutrient-rich surface mixed layer waters (Sautter & Thunell, 1991) associated with upwelling (e.g. Cullen & Prell, 1984; Anderson & Prell, 1991; Kroon *et al.* 1991; Naidu & Malmgren, 1996). In addition, *G. bulloides* has also been suggested to flourish in winter monsoon wind induced high surface productivity conditions (Singh *et al.* 2011, 2018). *N. dutertrei* is a eutrophic thermocline dwelling species (e.g. Ravelo *et al.* 1990; Ravelo & Fairbanks, 1992) and it dominates when nutrients are brought into the photic zone, enhancing the primary productivity (Fairbanks *et al.* 1982; Schiebel *et al.* 2001; Ishikawa & Oda, 2007). It calcifies within the thermocline in association with the chlorophyll maximum (Sautter & Thunell, 1991). In tropical areas, the abundance variation of *N. dutertrei* has been considered to be related to the changes in thermocline depth (Andreasen & Ravelo, 1997; Jian *et al.* 2000).

The interval between 1.85 Ma and 2.7 Ma was a period when surface water was more stratified and nutrient-poor (oligotrophic), resulting in overall low productivity. Today, the surface water hydrography and productivity conditions in the EAS are primarily influenced by the winter NE monsoonal wind, which invokes vertical mixing leading to injection of nutrients to the photic zone and thus increased seasonal winter productivity. By analogy to the modern conditions, we therefore infer that the winter monsoon circulation was generally weak during this time interval. Low average values of $\delta^{13}C$ also support our interpretation of low-productivity conditions during this period (Fig. 4). Heavier seawater oxygen isotope values compared to the time period 1.55–1.65 Ma might suggest that rainfall and/or continental runoff was lower during this period, indicating a weaker summer monsoon. Taken together, our faunal records, combined with the isotope data, suggest a weaker summer (SW) and winter (NE) monsoon during the time period 1.85–2.7 Ma. Our faunal, isotopic, Mg/Ca-based SST and seawater $\delta^{18}O$ records show a prominent shift between ~1.65 Ma and 1.85 Ma, which is interpreted to reflect a major reorganization of the South Asian / Indian monsoon circulation around that time (Fig. 4).

Overall higher absolute abundances of *G. glutinata*, *G. bulloides* and *N. dutertrei* between 1.55 Ma and 1.65 Ma are suggested to indicate nutrient-rich (eutrophic) and high-productivity surface water conditions due to intensification of the monsoonal winds (Fig. 4). On the other hand, the absolute abundance of *G. ruber*, which is a mixed layer species and usually associated with oligotrophic surface water conditions, also significantly increased during this period. In addition, average lighter seawater $\delta^{18}O$ values between 1.55 Ma and 1.65 Ma suggest increased freshening of surface waters, most likely associated with increased fresh-water runoff from the continent due to enhanced South Asian / Indian summer monsoon precipitation. However, a detailed comparison of our proxy records reveals that periods of heavier *G. sacculifer-quadrilobatus* $\delta^{18}O$ values and high relative abundances (%) of *G. glutinata* and *N. dutertrei* are associated with low relative abundances of *G. ruber* (Fig. 5). We submit that the *G. sacculifer-quadrilobatus* $\delta^{18}O$ record reveals glacial–interglacial variations for the interval 1.55–1.65 Ma because the amplitude of changes is similar to that found in the 'LR04' benthic $\delta^{18}O$ record stack for that time period (Lisiecki & Raymo, 2005). Although only fragmentary, our Mg/Ca-based SST record reveals a *c.* 3°C glacial/interglacial amplitude which is similar to that of the Holocene – Last Glacial Maximum amplitude in the EAS (Anand *et al.* 2008) (Fig. 5). We suggest that periods of high relative abundances of *G. glutinata* and *N. dutertrei* represent glacial periods with less stratified surface water, high nutrient levels and high productivity. We suggest that the enhanced productivity during those periods

https://doi.org/10.1017/S0016756819000098 Published online by Cambridge University Press

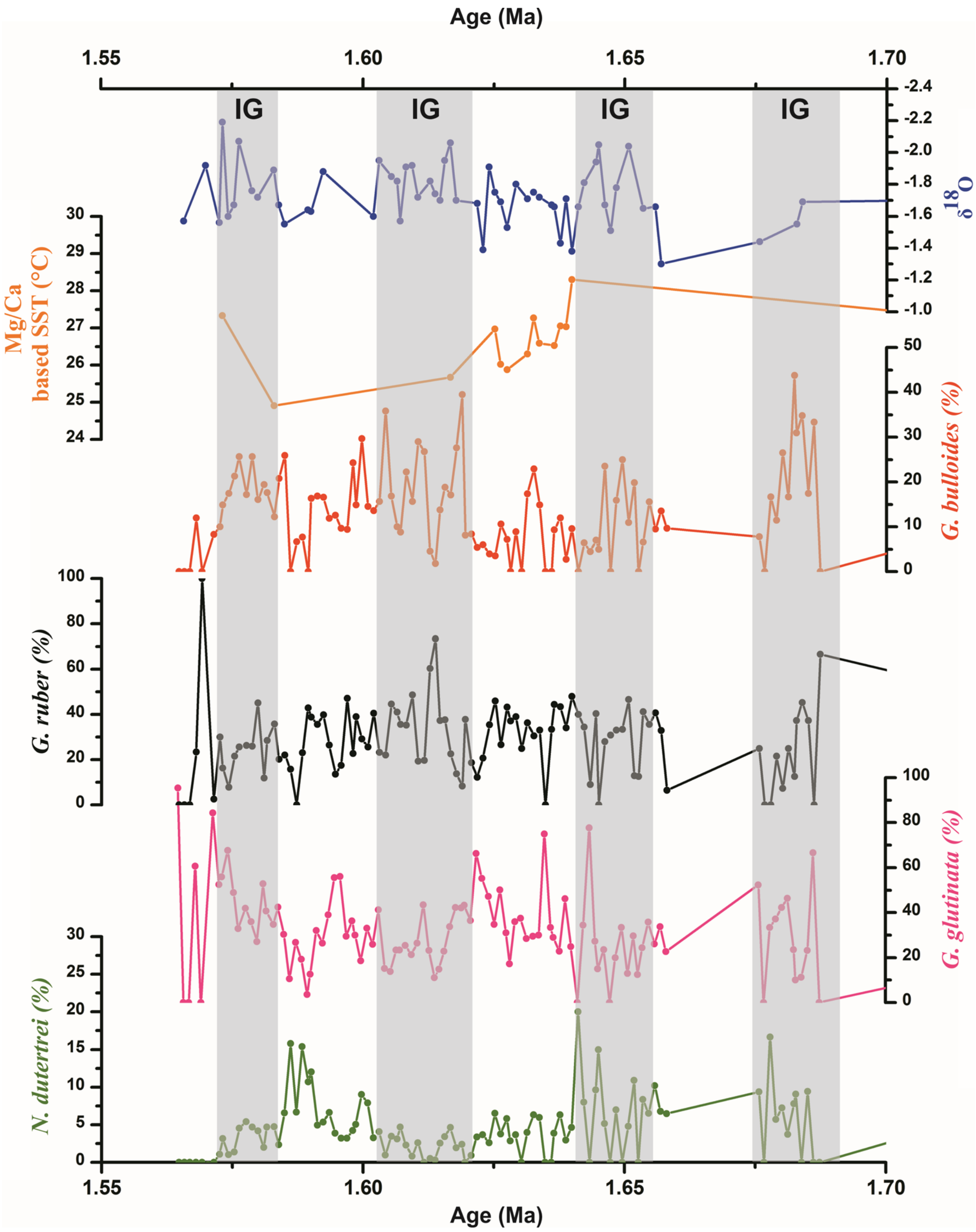

Fig. 5. Faunal, stable oxygen isotope and SST records for 1.55–1.7 Ma. Planktic foraminiferal (*N. dutertrei*, *G. glutinata*, *G. ruber* and *G. bulloides*) relative abundances, Mg/Ca-based SST record and $\delta^{18}O$ record of *G. sacculifer-quadrilobatus.* Dark bands represent interglacials (IG).

was triggered by the intensification of the NE winter monsoon winds. This assertion is based on the fact that present-day primary productivity changes in the EAS are strongly coupled to the intensity of the NE winter monsoon wind, affecting both SST and MLD in the Arabian Sea, and thus control the entrainment of nutrients into the mixed layer. A link between NE monsoon wind strength, SST and productivity has been observed in the northern Arabian Sea on glacial/interglacial timescales during the late Pleistocene (Rostek *et al.* 1997; Schulte *et al.* 1999; Schulte & Müller, 2001). The high productivity in the N and NE Arabian Sea during the glacial period has been related to the intensified NE monsoon winds inducing convective overturning and injection of nutrient-rich subsurface waters to the euphotic zone (Rostek *et al.* 1997; Reichart *et al.* 1998). Records of high productivity in the EAS during glacial stages of the late Pleistocene have also been attributed to the intensification of NE winter monsoon winds (e.g. Ivanova *et al.* 2003; Singh *et al.* 2006, 2011, 2018). Other studies have further suggested relatively low surface water productivity during interglacials, which were mainly caused by surface water stratification driven by high fluvial discharge/runoff from rivers flowing through the Western Ghats, mainly the Narmada and Tapti, when the SW monsoon was intensified and the NE monsoon circulation was weak (Singh *et al.* 2006, 2018; Cabarcos *et al.* 2014). In contrast, the surface water was more stratified and oligotrophic during periods when our planktic foraminifera stable oxygen isotope record reveals lighter values, which are most likely associated with interglacial periods (Fig. 5). It is intriguing to note that high abundances of *G. bulloides* occur during periods of lighter $\delta^{18}O$ values between 1.55 Ma and 1.65 Ma, which are interpreted to reflect interglacials (see above). We suggest that the SW summer

https://doi.org/10.1017/S0016756819000098 Published online by Cambridge University Press

monsoon was intensified during the interglacial periods and stronger upwelling appeared in the western Arabian Sea. Filaments of this upwelling probably reached the area of coring, resulting in a moderate increase in productivity and thus relatively higher abundances of *G. bulloides* during interglacial periods. In addition, a moderate increase in productivity might have been caused by enhanced fluvial runoff which supplied more nutrients to the EAS due to an interglacial strengthening of the SW summer monsoonal rainfall. However, the latter scenario cannot be fully proven by our datasets because our seawater $\delta^{18}O$ record (proxy for salinity and thus changes in monsoonal rainfall) is of low resolution (Fig. 4). In summary, our proxy records suggest an overall weaker NE and SW monsoon during 1.85–2.7 Ma, and an intensification of the NE and SW monsoon between 1.55 Ma and 1.65 Ma.

5.c. Monsoon dynamics during the early Pleistocene

Our proxy records of the studied section at IODP Site U1457 reveal changes in upper water column structure occurring between *c.* 1.65 Ma and 1.85 Ma, most likely due to an intensification of the winter South Asian / Indian monsoon circulation system. Our study suggests that prior to 1.85 Ma, NE monsoon circulation was generally weaker than after 1.65 Ma. After 1.65 Ma, higher magnitudes of variations in productivity, SST and surface water stratification / vertical mixing on glacial/interglacial scale are suggestive of the intensification of the NE monsoon. Indian / South Asian summer monsoon variations have been reconstructed using marine (biogenic and lithogenic indices from the Arabian Sea; Clemens *et al.* 1996) and continental (Heqing palaeolake, pollen, total organic carbon (TOC), geochemical proxies; An *et al.* 2011) records during the Pliocene–Pleistocene. A long-term decrease in the lithogenic grain-size fraction indicates that the persistent growth of the Northern Hemisphere (NH) ice sheets since 3.5 Ma has weakened the intensity of the Indian summer monsoon (Clemens *et al.* 1996). On glacial–interglacial timescales, the Heqing palaeolake record indicates the importance of interhemispheric forcing in driving Indian / South Asian summer monsoon variability at glacial–interglacial timescales (An *et al.* 2011). An *et al.* (2011) found a dominant NH forcing that results in large-amplitude fluctuations of the ISM variation when ISM minima were coincident with NH ice volume maxima after *c.* 1.82 Ma. Increasing NH glaciation decreases the strength of the Indian low, resulting in a weakening of the ISM with the growth of NH ice sheets (An *et al.* 2011). Although not conclusive, we suggest that increasing NH glaciations strengthened the NE (winter) winds, resulting in a higher magnitude of variations in productivity, SST and surface water stratification / vertical mixing after 1.65–1.85 Ma.

In addition, several studies have suggested drastic changes in atmospheric circulations in low- to mid-latitude regions since the mid-Pliocene (e.g. Jia *et al.* 2008; Etourneau *et al.* 2009; Trauth *et al.* 2009). Recent studies propose that the zonal and meridional atmospheric circulations (Walker Circulation and Hadley Cell), which are related to the E–W SST gradient along the equatorial Pacific, strengthened in the early Pleistocene after 2.2 Ma (e.g. Etourneau *et al.* 2010). Maximum E–W SST differences along the equatorial Pacific have been reported between 2.2 Ma and 1.5 Ma. A modern-like Walker Circulation with strong seasonality of the monsoon system was established during this period. This interpretation seems to be consistent with our findings and we could also assume that the strengthening of the Walker and Hadley circulations and the associated trade winds may have significantly amplified the intensity of the monsoonal winter winds in the EAS between 1.55 Ma and 1.65 Ma, resulting in the strengthening of surface water mixing and productivity.

6. Conclusions

Here we have presented the first evidence for changes in strength of the winter (NE) South Asian / Indian monsoon during the early Pleistocene. Based on the reconstruction of surface water conditions at IODP Site U1457 located in the EAS, we identified an intensification of the winter (NE) monsoon between 1.55 Ma and 1.65 Ma. This would probably have been initiated between ∼1.65 Ma and 1.85 Ma, associated with an increasing NH glaciation after *c.* 1.82 Ma. In addition, this major reorganization in South Asian / Indian monsoon circulation and intensification of the winter monsoon winds might be attributed to the development of strong meridional and zonal atmospheric circulations (i.e. Walker Circulation and Hadley Circulation). On the basis of our low-resolution records we cannot resolve the influence of interhemispheric forcing in driving the South Asian/winter monsoon variability at glacial and interglacial timescales during the early Pleistocene. Better-resolved sedimentary archives are needed to confirm and understand the evolution and development of the South Asian/winter monsoon during the early Pleistocene.

Author ORCIDs. Arun Deo Singh, 0000-0003-1287-8067.

Acknowledgements. Samples for this project were provided by the International Ocean Discovery Program. We are grateful to M. Mohtadi, J. Groeneveld and H. Kuhnert for supporting the isotope and trace element analyses. R.K.S. acknowledges CSIR for the Junior Research Fellowship. This study is also supported by the DST–PURSE Grant to A.D.S. We are grateful to the shipboard team (co-chief scientists, staff scientist and other scientists, technical staff and crew members on board *JOIDES Resolution*) of IODP Expedition 355. We thank the Editor and two anonymous reviewers for constructive comments and suggestions, which helped us to improve the manuscript. We also thank Pradyumna Singh for his help in identification of foraminifera, and Jayu Narvekar for preparation of the climatological maps.

References

An ZS, Clemens S, Shen J, Qiang X, Jin Z, Sun Y, Prell W, Luo J, Wang S, Xu H, Cai Y, Zhou W, Liu X, Liu W, Shi Z, Yan L, Xiao X, Chang H, Wu F, Ai L and Lu F (2011) Glacial-interglacial Indian summer monsoon dynamics. *Science* **333**, 719–23.

Anand P, Elderfield H and Conte M (2003) Calibration of Mg/Ca thermometry in planktonic foraminifera from a sediment trap time series. *Paleoceanography* **18**. doi: 10.1029/2002PA000846.

Anand P, Kroon D, Singh AD, Ganeshram R, Ganssen G and Elderfield H (2008) Coupled sea surface temperature-seawater $\delta^{18}O$ reconstructions in the Arabian Sea at the millennial scale for the last 35 ka. *Paleoceanography* **23**. doi: 10.1029/2007PA001564.

Anderson D and Prell W (1991) Coastal upwelling gradient during the late Pleistocene. In *Proceedings of the Ocean Drilling Program, Scientific Results* (eds WL Prell, N Niitsuma, ***et al.***), vol. **117**, pp. 265–76. College Station, Texas: Ocean Drilling Program.

Anderson D and Prell W (1993) A 300 kyr record of upwelling off Oman during the Late Quaternary: evidence of the Asian southwest monsoon. *Paleoceanography* **8**, 193–208.

Andreasen D and Ravelo A (1997) Tropical Pacific Ocean thermocline depth reconstructions for the Last Glacial Maximum. *Paleoceanography* **12**, 395–413.

Banakar V, Oba T, Chodankar A, Kuramoto T, Yamamoto M and Minagawa M (2005) Monsoon related changes in sea surface productivity and water column denitrification in the Eastern Arabian Sea during the last glacial cycle. *Marine Geology* **219**, 99–108.

Banse K (1984) Overview of the hydrography and associated biological phenomena in the Arabian Sea off Pakistan. In *Marine Geology and Oceanography of Arabian Sea and Coastal Pakistan* (eds J Haq and B Milliman), pp. 271–303. New York: Van Nostrand Reinhold.
Banse K (1987) Seasonality of phytoplankton chlorophyll in the central and northern Arabian sea. *Deep Sea Research Part A. Oceanographic Research Papers* **34**, 713–23.
Banse K and McClain C (1986) Winter blooms of phytoplankton in the Arabian Sea as observed by the Coastal Zone Color Scanner. *Marine Ecology Progress Series* **34**, 201–11.
Barker S, Greaves M and Elderfield H (2003) A study of cleaning procedures used for foraminiferal Mg/Ca paleothermometry. *Geochemistry, Geophysics, Geosystems* **4**. doi: 10.1029/2003GC000559.
Bemis B, Spero H, Bijma J and Lea D (1998) Reevaluation of the oxygen isotopic composition of planktonic foraminifera: experimental results and revised paleotemperature equations. *Paleoceanography* **13**, 150–60.
Berger W (1973) Deep-sea carbonates; Pleistocene dissolution cycles. *The Journal of Foraminiferal Research* **3**, 187–95.
Bintanja R and Van de Wal R (2008) North American ice-sheet dynamics and the onset of 100,000-year glacial cycles. *Nature* **454**, 869–72.
Brock J, Sathyendranath S and Platt T (1994) A model study of seasonal mixed-layer primary production in the Arabian Sea. *Proceedings of the Indian Academy of Sciences – Earth and Planetary Sciences* **103**, 163–76.
Cabarcos E, Flores J, Singh AD and Sierro F (2014) Monsoonal dynamics and evolution of the primary productivity in the eastern Arabian Sea over the past 30 ka. *Palaeogeography, Palaeoclimatology, Palaeoecology* **411**, 249–56.
Cayre O and Bard E (1999) Planktonic foraminiferal and alkenone records of the last deglaciation from the eastern Arabian Sea. *Quaternary Research* **52**, 337–42.
Chodankar A, Banakar V and Oba T (2005) Past 100 ky surface salinity-gradient response in the Eastern Arabian Sea to the summer monsoon variation recorded by δ^{18}O of G. sacculifer. *Global and Planetary Change* **47**, 135–42.
Clemens S, Murray D and Prell W (1996) Nonstationary phase of the plio-Pleistocene Asian monsoon. *Science* **274**, 943–8.
Clemens S, Prell W, Murray D, Shimmield G and Weedon G (1991) Forcing mechanisms of the Indian Ocean monsoon. *Nature* **353**, 720–5.
Conan S and Brummer G (2000) Fluxes of planktic foraminifera in response to monsoonal upwelling on the Somalia Basin margin. *Deep Sea Research Part II: Topical Studies in Oceanography* **47**, 2207–27.
Conan S, Ivanova E and Brummer G (2002) Quantifying carbonate dissolution and calibration of foraminiferal dissolution indices in the Somali Basin. *Marine Geology* **182**, 325–49.
Cullen J and Prell W (1984) Planktonic foraminifera of the northern Indian Ocean: distribution and preservation in surface sediments. *Marine Micropaleontology* **9**, 1–52.
Etourneau J, Martinez P, Blanz T and Schneider R (2009) Pliocene-Pleistocene variability of upwelling activity, productivity, and nutrient cycling in the Benguela region. *Geology* **37**, 871–4.
Etourneau J, Schneider R, Blanz T and Martinez P (2010) Intensification of the Walker and Hadley atmospheric circulations during the Pliocene-Pleistocene climate transition. *Earth and Planetary Science Letters* **297**, 103–10.
Fairbanks R, Sverdlove M, Free R, Wiebe P and Bé A (1982) Vertical distribution and isotopic fractionation of living planktonic foraminifera from the Panama Basin. *Nature* **298**, 841–4.
Gupta A, Anderson D and Overpeck J (2003) Abrupt changes in the Asian southwest monsoon during the Holocene and their links to the North Atlantic Ocean. *Nature* **421**, 354–7.
Guptha M, Naidu P, Haake B and Schiebel R (2005) Carbonate and carbon fluctuations in the Eastern Arabian Sea over 140 ka: implications on productivity changes? *Deep Sea Research Part II: Topical Studies in Oceanography* **52**, 1981–93.
Hemleben C, Spindler M and Anderson O (1989) *Modern Planktonic Foraminifera*. Berlin: Springer-Verlag, 363 pp.
Hutson WH and Prell WL (1980) A paleoecological transfer function, FI-2, for Indian Ocean planktonic foraminifera. *Journal of Paleontology* **54**, 381–99.
Ishikawa S and Oda M (2007) Reconstruction of Indian monsoon variability over the past 230,000 years: planktic foraminiferal evidence from the NW Arabian Sea open-ocean upwelling area. *Marine Micropaleontology* **63**, 143–54.
Ivanochko T, Ganeshram R, Brummer G, Ganssen G, Jung S, Moreton S and Kroon D (2005) Variations in tropical convection as an amplifier of global climate change at the millennial scale. *Earth and Planetary Science Letters* **235**, 302–14.
Ivanova E, Schiebel R, Singh AD, Schmiedl G, Niebler H and Hemleben C (2003) Primary production in the Arabian Sea during the last 135 000 years. *Palaeogeography, Palaeoclimatology, Palaeoecology* **197**, 61–82.
Jia G, Chen F and Peng P (2008) Sea surface temperature differences between the western equatorial Pacific and northern South China Sea since the Pliocene and their paleoclimatic implications. *Geophysical Research Letters* **35**, L18609. doi: 10.1029/2008GL034792.
Jian Z, Wang P, Chen M, Li B, Zhao Q, Bühring C, Laj C, Lin H, Pflaumann U, Bian Y, Wang R and Cheng X (2000) Foraminiferal responses to major Pleistocene paleoceanographic changes in the southern South China Sea. *Paleoceanography* **15**, 229–43.
Jung S, Ivanova E, Reichart G, Davies G, Ganssen G, Kroon D and Van Hinte J (2002) Centennial-millennial-scale monsoon variations off Somalia over the last 35 ka. In *The Tectonic and Climatic Evolution of the Arabian Sea Region* (eds PD Clift, D Kroon, C Gaedicke and J Craig), pp. 341–52. Geological Society of London, Special Publication no. 195.
Kennett JP and Srinivasan MS (1983) *Neogene Planktonic Foraminifera: A Phylogenetic Atlas*. Stroudsburg: Hutchinson Ross Publishing Company, 265 pp.
Koné V, Aumont O, Lévy M and Resplandy L (2009) Physical and biogeochemical controls of the phytoplankton seasonal cycle in the Indian Ocean: a modeling study. In *Indian Ocean Biogeochemical Processes and Ecological Variability* (eds JD Wiggert, RR Hood, S Wajih, A Naqvi, KH Brink & SL Smith), pp. 147–66. Washington, DC: American Geophysical Union, Geophysical Monograph no. 185.
Kroon D, Steens T and Troelstra S (1991) Onset of monsoonal related upwelling in the western Arabian Sea as revealed by planktonic foraminifers. In *Proceedings of the Ocean Drilling Program, Scientific Results* (eds WL Prell, N Niitsuma *et al.*) vol. **117**, pp. 257–63. College Station, Texas: Ocean Drilling Program.
Lévy M, Shankar D, André J, Shenoi S, Durand F and De Boyer Montégut C (2007) Basin-wide seasonal evolution of the Indian Ocean's phytoplankton blooms. *Journal of Geophysical Research* **112**, C12. doi: 10.1029/2007JC004090.
Lisiecki L and Raymo M (2005) A Pliocene-Pleistocene stack of 57 globally distributed benthic δ^{18}O records. *Paleoceanography* **20**, PA1003. doi: 10.1029/2004PA001071.
Luis A and Kawamura H (2004) Air-sea interaction, coastal circulation and primary production in the eastern Arabian Sea: a review. *Journal of Oceanography* **60**, 205–18.
Madhupratap M, Kumar S, Bhattathiri P, Kumar M, Raghukumar S, Nair K and Ramaiah N (1996) Mechanism of the biological response to winter cooling in the northeastern Arabian Sea. *Nature* **384**, 549–52.
Mohtadi M, Prange M, Oppo D, De Pol-Holz R, Merkel U, Zhang X, Steinke S and Lückge A (2014) North Atlantic forcing of tropical Indian Ocean climate. *Nature* **509**, 76–80.
Naidu P and Malmgren B (1996) A high-resolution record of Late Quaternary upwelling along the Oman Margin, Arabian Sea based on planktonic foraminifera. *Paleoceanography* **11**, 129–40.
Pandey D, Clift P, Kulhanek D and Expedition 355 Scientists (2015) Expedition 355 preliminary report: Arabian Sea Monsoon. *Proceedings of the International Ocean Discovery Program* **2015**, 1–46.
Pandey D, Clift P, Kulhanek D and Expedition 355 Scientists (2016) Site U1457. *Proceedings of the International Ocean Discovery Program* **2016**, 1–49.
Pattan J, Masuzawa T, Naidu P, Parthiban G and Yamamoto M (2003) Productivity fluctuations in the southeastern Arabian Sea during the last 140 ka. *Palaeogeography, Palaeoclimatology, Palaeoecology* **193**, 575–90.
Peeters F and Brummer G (2002) The seasonal and vertical distribution of living planktic foraminifera in the NW Arabian Sea. In *The Tectonic and Climatic Evolution of the Arabian Sea Region* (eds PD Clift, D Kroon, C

https://doi.org/10.1017/S0016756819000098 Published online by Cambridge University Press

Gaedicke and J Craig), pp. 463–97. Geological Society of London, Special Publication no. 195.

Prasanna Kumar S, Narvekar J, Kumar A and Shaji C (2004) Intrusion of the Bay of Bengal water into the Arabian Sea during winter monsoon and associated chemical and biological response. *Geophysical Research Letters* **31**, L15304. doi: 10.1029/2004GL020247.

Rao R, Molinari R and Festa J (1989) Evolution of the climatological near-surface thermal structure of the tropical Indian Ocean: 1. Description of mean monthly mixed layer depth, and sea surface temperature, surface current, and surface meteorological fields. *Journal of Geophysical Research* **94**, 10,801–15.

Ravelo A and Fairbanks R (1992) Oxygen isotopic composition of multiple species of planktonic foraminifera: recorders of the modern photic zone temperature gradient. *Paleoceanography* **7**, 815–31.

Ravelo A, Fairbanks R and Philander S (1990) Reconstructing tropical Atlantic hydrography using planktontic foraminifera and an ocean model. *Paleoceanography* **5**, 409–31.

Reichart G, Lourens L and Zachariasse W (1998) Temporal variability in the northern Arabian Sea oxygen minimum zone (OMZ) during the last 225,000 years. *Paleoceanography* **13**, 607–21.

Rixen T, Haake B and Ittekkot V (2000) Sedimentation in the western Arabian Sea: the role of coastal and open-ocean upwelling. *Deep Sea Research Part II: Topical Studies in Oceanography* **47**, 2155–78.

Rostek F, Bard E, Beaufort L, Sonzogni C and Ganssen G (1997) Sea surface temperature and productivity records for the past 240 kyr in the Arabian Sea. *Deep Sea Research Part II: Topical Studies in Oceanography* **44**, 1461–80.

Sautter L and Thunell R (1991) Planktonic foraminiferal response to upwelling and seasonal hydrographic conditions; sediment trap results from San Pedro Basin, Southern California Bight. *The Journal of Foraminiferal Research* **21**, 347–63.

Schiebel R, Waniek J, Bork M and Hemleben C (2001) Planktic foraminiferal production stimulated by chlorophyll redistribution and entrainment of nutrients. *Deep Sea Research Part I: Oceanographic Research Papers* **48**, 721–40.

Schott F (1983) Monsoon response of the Somali current and associated upwelling. *Progress in Oceanography* **12**, 357–81.

Schott F and McCreary J (2001) The monsoon circulation of the Indian Ocean. *Progress in Oceanography* **51**, 1–123.

Schulte S and Müller P (2001) Variations of sea surface temperature and primary productivity during Heinrich and Dansgaard-Oeschger events in the northeastern Arabian Sea. *Geo-Marine Letters* **21**, 168–75.

Schulte S, Rostek F, Bard E, Rullkötter J and Marchal O (1999) Variations of oxygen-minimum and primary productivity recorded in sediments of the Arabian Sea. *Earth and Planetary Science Letters* **173**, 205–21.

Schulz H, Von Rad U and Erlkeuser H (1998) Correlation between Arabian Sea and Greenland climate oscillations of the past 110,000 years. *Nature* **393**, 54–7.

Schulz H, Von Rad U and Ittekkot V (2002) Planktic foraminifera, particle flux and oceanic productivity off Pakistan, NE Arabian Sea: modern analogues and application to the palaeoclimatic record. In *The Tectonic and Climatic Evolution of the Arabian Sea Region* (eds PD Clift, D Kroon, C Gaedicke and J Craig), pp. 499–516. Geological Society of London, Special Publication no. 195.

Shankar D, Remya R, Vinayachandran P, Chatterjee A and Behera A (2015) Inhibition of mixed-layer deepening during winter in the northeastern Arabian Sea by the West India Coastal Current. *Climate Dynamics* **47**, 1049–72.

Shetye S, Gouveia A, Shenoi S, Michael G, Sundar D, Almeida A and Santanam K (1991) The coastal current off western India during the northeast monsoon. *Deep Sea Research Part A. Oceanographic Research Papers* **38**, 1517–29.

Singh AD, Jung S, Anand P, Kroon D and Ganeshram R (2018) Rapid switch in monsoon-wind induced surface hydrographic conditions of the eastern Arabian Sea during the last deglaciation. *Quaternary International* **479**, 3–11.

Singh AD, Jung S, Darling K, Ganeshram R, Ivanochko T and Kroon D (2011) Productivity collapses in the Arabian Sea during glacial cold phases. *Paleoceanography* **26**, PA3210. doi: 10.1029/2009PA001923.

Singh AD, Kroon D and Ganeshram R (2006) Millennial scale variations in productivity and OMZ intensity in the eastern Arabian Sea. *Journal of the Geological Society of India* **68**, 369–77.

Steens T, Ganssen G and Kroon D (1992) Oxygen and carbon isotopes in planktonic foraminifera as indicators of upwelling intensity and upwelling-induced high productivity in sediments from the northwestern Arabian Sea. In *Upwelling System Evolution since the Early Miocene* (eds CP Summerhayes, WL Prell and KC Emeis), pp. 107–19. Geological Society of London, Special Publication no. 64.

Thamban M, Purnachandra Rao V, Schneider R and Grootes P (2001) Glacial to Holocene fluctuations in hydrography and productivity along the southwestern continental margin of India. *Palaeogeography, Palaeoclimatology, Palaeoecology* **165**, 113–27.

Trauth M, Larrasoaña J and Mudelsee M (2009) Trends, rhythms and events in Plio-Pleistocene African climate. *Quaternary Science Reviews* **28**, 399–411.

Vénec-Peyré M, Caulet J and Grazzini C (1995) Paleohydrographic changes in the Somali Basin (5°N upwelling and equatorial areas) during the last 160 kyr, based on correspondence analysis of foraminiferal and radiolarian assemblages. *Paleoceanography* **10**, 473–91.

Vijith V, Vinayachandran P, Thushara V, Amol P, Shankar D and Anil A (2016) Consequences of inhibition of mixed-layer deepening by the West India Coastal Current for winter phytoplankton bloom in the northeastern Arabian Sea. *Journal of Geophysical Research: Oceans* **121**, 6583–603.

Von Rad U, Schulz H, Riech V, Den Dulk M, Berner U and Sirocko F (1999) Multiple monsoon-controlled breakdown of oxygen-minimum conditions during the past 30,000 years documented in laminated sediments off Pakistan. *Palaeogeography, Palaeoclimatology, Palaeoecology* **152**, 129–61.

https://doi.org/10.1017/S0016756819000098 Published online by Cambridge University Press